

# Muon spin relaxation in mixed perovskite (LaAlO<sub>3</sub>)<sub>x</sub>(SrAl<sub>0.5</sub>Ta<sub>0.5</sub>O<sub>3</sub>)<sub>1-x</sub> with $x \simeq 0.3$

Takashi U. Ito<sup>1\*</sup>, Wataru Higemoto<sup>1,2</sup>, Akihiro Koda<sup>3</sup>,  
Junpei G. Nakamura<sup>3</sup>, Koichiro Shimomura<sup>3</sup>

<sup>1\*</sup>Advanced Science Research Center, Japan Atomic Energy Agency,  
Tokai, Ibaraki, 319-1195, Japan.

<sup>2</sup>Department of Physics, Tokyo Institute of Technology, Meguro, Tokyo,  
152-8551, Japan.

<sup>3</sup>Institute of Materials Structure Science, High Energy Accelerator  
Research Organization (KEK), Tsukuba, Ibaraki, 305-0801, Japan.

\*Corresponding author(s). E-mail(s): [tuito@post.j-parc.jp](mailto:tuito@post.j-parc.jp);

## Abstract

We report on muon spin relaxation ( $\mu^+$ SR) measurements in a mixed perovskite compound, (LaAlO<sub>3</sub>)<sub>x</sub>(SrAl<sub>0.5</sub>Ta<sub>0.5</sub>O<sub>3</sub>)<sub>1-x</sub> with  $x \simeq 0.3$  (LSAT), which is widely used as a single-crystalline substrate for thin film deposition. In zero applied field (ZF), muon depolarization due to the distribution of nuclear dipole fields was observed in the temperature range from 4 K to 270 K. Interestingly,  $\mu^+$ SR time spectra in ZF maintained a Gaussian-like feature over the entire range, while the depolarization rate exhibited a monotonic decrease with increasing temperature. This behavior may be attributed to the thermally activated diffusion of muons between a few adjacent sites within a confined space of the angstrom scale, where the motionally averaged local field that each muon experiences can remain non-zero and result in maintaining the Gaussian-like line shape. The spatial distribution of electrostatic potential at lattice interstices evaluated via density functional theory calculations suggests that such a restriction of muon diffusion paths can be caused by the random distribution of cations with different nominal valences in the mixed perovskite lattice.

**Keywords:** Muon diffusion, LSAT, mixed perovskite oxide, substrate for thin-film deposition

# 1 Introduction

The ultra-slow muon beamline (U-line), currently under commissioning at the Materials and Life Science Experimental Facility in the Japan Proton Accelerator Research Complex (J-PARC), enables positive muons ( $\mu^+$ ) to be implanted into thin-film materials for  $\mu^+$  spin rotation and relaxation ( $\mu^+$ SR) spectroscopy with nanometer depth resolution [1]. The  $\mu^+$ SR spectrometer for the U-line is in the final stages of tune-ups and is expected to become available to public users shortly.

In anticipation of forthcoming  $\mu^+$ SR experiments using ultra-slow muons, we have investigated  $\mu^+$ SR signals from typical substrate materials, which can be superposed on those from thin-film samples deposited on the substrates. In this paper, we specifically focus on a mixed perovskite substrate material,  $(\text{LaAlO}_3)_x(\text{SrAl}_{0.5}\text{Ta}_{0.5}\text{O}_3)_{1-x}$  with  $x \simeq 0.3$  (LSAT) [2]. LSAT is obtained as a solid solution of  $\text{LaAlO}_3$  and  $\text{SrAl}_{0.5}\text{Ta}_{0.5}\text{O}_3$  and has a cubic  $\text{ABO}_3$  perovskite structure at the molar ratio of  $\sim 3:7$ . The  $A$  and  $B$  cation sites are statistically occupied by  $\text{Sr}^{2+}$  and  $\text{La}^{3+}$ , and  $\text{Al}^{3+}$  and  $\text{Ta}^{5+}$ , respectively. Single-crystalline substrates of LSAT were developed to overcome difficulties found in  $\text{LaAlO}_3$  substrates, such as twinning, strain, and non-isotropic microwave properties [3], and have been widely used for the epitaxial growth of various thin films, primarily of perovskite-related materials [3–7] and GaN semiconductors [8].

In this paper, we report  $\mu^+$ SR measurements on LSAT in zero applied field (ZF) below room temperature. We also present the results of density functional theory (DFT) calculations for an approximate model of LSAT, which were performed to gain deeper insight into the localization site and kinetics of muons in the mixed perovskite lattice.

## 2 Materials and methods

LSAT single crystals of  $10 \times 10 \times 0.5 \text{ mm}^3$  were obtained from CRYSTAL GmbH, Germany. These single crystals were grown by the Czochralski method and cut along the cubic (001) plane. Time-differential  $\mu^+$ SR experiments were performed at J-PARC using a spin-polarized surface muon beam in a longitudinal field configuration, with its initial polarization direction nominally parallel to the beam axis. The ARTEMIS spectrometer [9] at the S1 area of the Materials and Life Science Experimental Facility was used with a conventional  $^4\text{He}$  flow cryostat for the ZF- $\mu^+$ SR measurements of LSAT in the temperature range from 4 K to 270 K. Four single crystals of LSAT were mounted on a silver sample holder with the (001) plane perpendicular to the beam axis. The asymmetry of  $\mu^+$  decay,  $A$ , was monitored by the “Forward” and “Backward” positron counters as a function of the elapsed time  $t$  from the instant of muon implantation.

All DFT calculations were performed using the QUANTUM ESPRESSO package [10, 11]. The generalized gradient approximation using Perdew-Burke-Ernzerhof (PBE) exchange correlation functional was adopted. Projector augmented-wave potentials with La(4*f*, 5*s*, 5*p*, 5*d*, 6*s*, 6*p*), Sr(4*s*, 4*p*, 5*s*, 5*p*), Al(3*s*, 3*p*), Ta(5*s*, 5*p*, 5*d*, 6*s*) and O(2*s*, 2*p*) valence states were used. Hubbard  $U$  corrections were applied to the La 4*f* and Ta 5*d* states using typical  $U_{eff}$  or  $U - J$  values listed in Ref. [12]. Electron

wave functions were expanded in plane waves with a cutoff of 70 Ry for kinetic energy and 600 Ry for charge density.

The LSAT structure was simulated within a  $3 \times 3 \times 3$  supercell of the five-atom cubic primitive cell. The supercell was composed of 7 La, 20 Sr, 17 Al, 10 Ta, and 81 O atoms so that it maintains total charge neutrality and approximates the chemical composition of our sample ( $\text{La}_{0.26}\text{Sr}_{0.76}\text{Al}_{0.61}\text{Ta}_{0.37}\text{O}_3$  according to the crystal manufacture-supplied data sheet [13]) well. To simulate the random cation distribution in LSAT, a special quasi-random structure (SQS) was generated using the Alloy Theoretic Automated Toolkit (ATAT) [14] and applied to the supercell.

Brillouin zone sampling with a Monkhorst-Pack  $\mathbf{k}$ -point mesh of  $2 \times 2 \times 2$  and Gaussian smearing with a broadening of 0.01 Ry were applied for structure optimization calculations using the pw.x module in the QUANTUM ESPRESSO package. Atomic positions were relaxed, while the lattice constant for the supercell was kept fixed at 11.604Å, according to the experimental lattice constant reported in the crystal manufacture-supplied data sheet [13]. Atomic forces were converged to within  $7.7 \times 10^{-3}$  eV/Å in the optimization process.

The spatial distribution of electrostatic potential in the optimized supercell was calculated using the pp.x module. It should be noted that the supercell does not involve any muon equivalent, and therefore the following discussion about the stability of muons at lattice interstices is simply based on a local electric field approximation.

We also evaluated the spatial distribution of  $\gamma_\mu\sigma$  in the optimized supercell via a dipolar sum calculation, where  $\gamma_\mu$  is the muon gyromagnetic ratio and  $\sigma$  is the root-mean-square width of the nuclear dipole field distribution at a given point. Through this calculation, both the experimental geometry using the single-crystalline sample and the effect of  $\mu^+$ -induced electric quadrupole interactions on nearest neighbor nuclei at cation sites were taken into account [15].

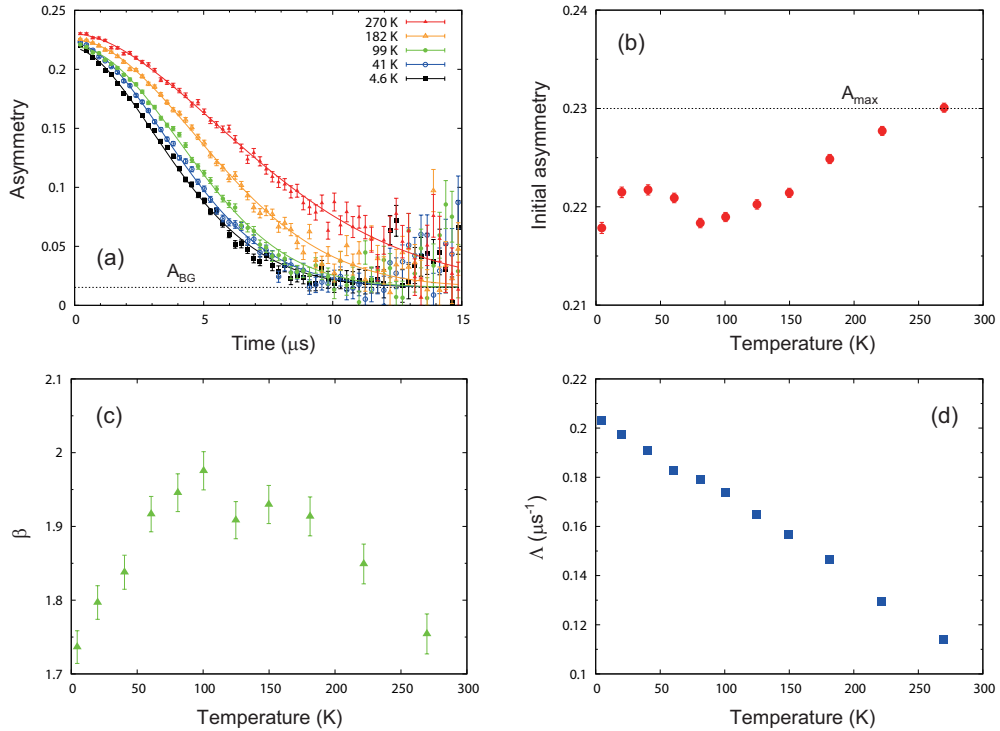
### 3 Results and discussion

Figure 1(a) shows ZF- $\mu^+$ SR spectra,  $A(t)$ , at 4.6, 41, 99, 182, and 270 K, representing the depolarization of implanted muons through interactions with surrounding nuclear spins. To capture the characteristics of the temperature variation, the following function was used to parameterize the spectra, i.e.,

$$A(t) = A_s \exp(-(\Lambda t)^\beta) + A_{\text{BG}}, \quad (1)$$

where  $A_s$  and  $A_{\text{BG}}$  are partial asymmetries from muons stopped in the sample and the silver sample holder, respectively,  $\Lambda$  is the depolarization rate, and  $\beta$  is the exponent. The magnitude of  $A_{\text{BG}}$  was determined using a reference sample (holmium) with similar geometry to the LSAT sample. The temperature dependencies of initial asymmetry ( $A_s + A_{\text{BG}}$ ),  $\beta$ , and  $\Lambda$  are shown in Figs. 1(b) to (d).

The initial asymmetry is close to the device-specific maximum value  $A_{\text{max}}$  of 0.23, suggesting that muons implanted into LSAT are predominantly found in diamagnetic environments. A small missing fraction at low temperatures may be associated with metastable paramagnetic species formed upon high energy implantation of muons, which were also observed in other transition-metal oxide insulators [16–20]. In this



**Fig. 1** (a) ZF- $\mu^+$ SR spectra at 4.6, 41, 99, 182, and 270 K. (b) to (d) Temperature dependencies of initial asymmetry ( $A_s + A_{BG}$ ),  $\beta$ , and  $\Lambda$ .

paper, we focus on the main diamagnetic component and do not elaborate further on the small paramagnetic fraction.

The Gaussian-like line shape observed at 4.6 K suggests that muons are quasi-static in the  $\mu^+$ SR time window ( $\sim 10^{-5}$  s) at low temperatures. Interestingly, the Gaussian-like feature is maintained up to room temperature (Fig. 1(c)), while the depolarization rate monotonically decreases with increasing temperature (Fig. 1(d)), suggesting the onset of muon diffusion. This is in sharp contrast to the depolarization behavior that is characteristic of global muon diffusion in homogeneous dense nuclear spin systems, as described by the dynamical Gaussian Kubo-Toyabe function [15, 21, 22]. The motional narrowing that preserves the Gaussian-like line shape can occur when the autocorrelation function of the nuclear dipole field experienced by muons has a long-time correlation term [23]. Such a situation can be realized not only when muons simultaneously observe diffusing and static ions with non-zero nuclear dipole moments at fixed sites [23], but also when each muon locally jumps between a few adjacent sites in a confined space of the angstrom scale. The local hopping picture may be justified in the LSAT lattice because the random distribution of four cations with different nominal valences can cause a large modulation in electrostatic potential at the electron-volt scale, which significantly limits the space where muons can diffuse.

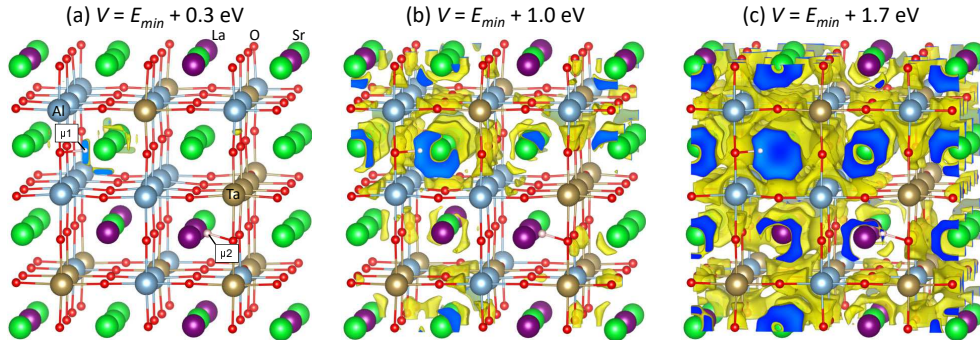


**Fig. 2** Isosurfaces for electrostatic potential  $V$  in the  $3 \times 3 \times 3$  SQS supercell of LSAT at (a)  $E_{min} + 0.3$  eV, (b)  $E_{min} + 1.0$  eV, and (c)  $E_{min} + 1.7$  eV, drawn with yellow curved surfaces with bluish cross sections. The smallest spheres labeled  $\mu 1$  and  $\mu 2$  exhibit the minimum energy position at  $E_{min}$  and a representative high energy position at  $E_{min} + 1.6$  eV, respectively.

The electrostatic potential  $V$ , calculated for the SQS model of LSAT, further justifies the local hopping picture. Figure 2 exhibits the isosurfaces at (a)  $V = E_{min} + 0.3$  eV, (b)  $V = E_{min} + 1.0$  eV, and (c)  $V = E_{min} + 1.7$  eV in the  $3 \times 3 \times 3$  SQS supercell, where  $E_{min}$  is the global minimum energy. Local minima in  $V$  are found at interstitial positions approximately  $1 \text{ \AA}$  away from nearest neighbor O in  $BO_2$  planes, which are consistent with  $\mu^+$  sites identified in other perovskite oxides [19, 20, 22, 24, 25]. The A and B cation sites around the minimum energy position ( $\mu 1$ ) with  $V = E_{min}$  are mainly filled with  $\text{Sr}^{2+}$  and  $\text{Al}^{3+}$ , respectively, whereas  $V$  is even higher by 1.6 eV at a representative oxygen-bound position ( $\mu 2$ ) surrounded by  $\text{La}^{3+}$  and  $\text{Ta}^{5+}$  cations. This is perfectly in line with the intuition that positively charged muons tend to avoid interstitial positions close to  $\text{La}^{3+}$  at the A site or  $\text{Ta}^{5+}$  at the B site with relatively large nominal valences.

The evolution of the volume enclosed by the isosurfaces of  $V$  from Fig. 2(a) to (c) suggests that muon diffusion paths are significantly restricted and isolated below room temperature, although they could expand with further increasing temperature through their interconnection. This implies that global muon diffusion is substantially inactive below 300 K in LSAT, in sharp contrast to the situation in a homogeneous  $\text{KTaO}_3$  lattice, where global diffusion was observed even below room temperature [22].

Finally, we discuss the consistency between the static line width  $\gamma_{\mu\sigma}$  calculated for the SQS model and the experimental value of  $\Lambda$ . Figure 3 shows the isosurface for  $\gamma_{\mu\sigma} = 0.20 \mu\text{s}^{-1}$  in the  $3 \times 3 \times 3$  SQS supercell of LSAT, which corresponds to  $\Lambda$  at  $T \rightarrow 0$  K (Fig. 1(d)). Oxygen-bound positions surrounded by  $\text{Sr}^{2+}$  and  $\text{Al}^{3+}$ , which are represented by the  $\mu 1$  site with  $\gamma_{\mu\sigma} = 0.183 \mu\text{s}^{-1}$  and  $V = E_{min}$ , are close to the  $0.20\text{-}\mu\text{s}^{-1}$  isosurface. On the other hand, those surrounded by  $\text{La}^{3+}$  and  $\text{Ta}^{5+}$  with much higher  $V$  are slightly off the isosurface, as evidenced by the smaller value of  $\gamma_{\mu\sigma} = 0.143 \mu\text{s}^{-1}$  at the  $\mu 2$  site. Since  $V$  at the  $\mu 2$  site is 1.6 eV higher than that at the  $\mu 1$  site, it is unlikely that the decrease in  $\Lambda$  toward room temperature is mainly caused by an increase in the relative occupancy of such high  $V$  sites with smaller  $\gamma_{\mu\sigma}$ s. It seems more plausible that the thermal activation of the local muon hopping

between a few oxygen-bound sites surrounded by  $\text{Sr}^{2+}$  and  $\text{Al}^{3+}$ , such as the  $\mu 1$  site, would cause the decrease in  $\Lambda$ .

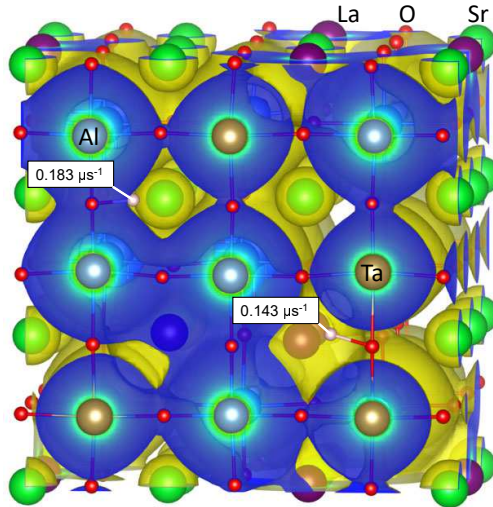


**Fig. 3** Isosurface for  $\gamma_{\mu}\sigma = 0.20 \mu\text{s}^{-1}$  in the  $3\times 3\times 3$  SQS supercell of LSAT, drawn with yellow curved surfaces with bluish cross sections.

## 4 Conclusions

In summary, we performed ZF- $\mu^+$ SR measurements on LSAT mixed-perovskite single crystals. Muon depolarization due to the distribution of nuclear dipole fields was observed in the temperature range from 4 K to 270 K. While the  $\mu^+$ SR time spectrum maintained a Gaussian-like feature over the entire range, the depolarization rate  $\Lambda$  exhibited a monotonic decrease with increasing temperature. This behavior may be attributed to the thermally activated diffusion of muons between a few adjacent sites within a confined space of the angstrom scale (local hopping), where the motionally averaged local field that each muon feels can remain non-zero and result in maintaining the Gaussian-like line shape. The spatial distribution of electrostatic potential  $V$  at lattice interstices evaluated via DFT calculations suggests that such a restriction of muon diffusion paths can be caused by the random distribution of cations with different nominal valences in the mixed perovskite lattice.

In terms of applications, LSAT is widely used as a single-crystalline substrate for the epitaxial growth of thin films. In  $\mu^+$ SR investigations of thin films deposited on the LSAT substrate using ultra-slow muons at J-PARC or low-energy muons at the Paul Scherrer Institut, attention must be paid to the contamination of the temperature-dependent signal from the substrate.

**Acknowledgments.** We thank the staff of the J-PARC muon facility for technical assistance. The DFT calculations were conducted with the supercomputer HPE SGI8600 in Japan Atomic Energy Agency. This research was partially supported by

Grants-in-Aid (Nos. 23K11707, 21H05102, 20K12484, 20H01864, and 20H02037) from the Japan Society for the Promotion of Science.

**Author contributions.** T.U.I. conceived the study, performed the  $\mu^+$ SR experiment in collaboration with W.H., A.K., J.G.N., and K.S., conducted data analysis and DFT calculations, and wrote the manuscript. All authors participated in the review and editing of the manuscript.

## References

- [1] Kanda, S., Teshima, N., Adachi, T., Ikedo, Y., Miyake, Y., Nagatani, Y., Nakamura, S., Oishi, Y., Shimomura, K., Strasser, P., Umezawa, T.: The ultra-slow muon beamline at J-PARC: present status and future prospects. *J. Phys.: Conf. Ser.* **2462**, 012030 (2023)
- [2] Mateika, D., Kohler, H., Laudan, H., Völkel, E.: Mixed-perovskite substrates for high- $T_c$  superconductors. *J. Cryst. Growth* **109**, 447–456 (1991)
- [3] Tidrow, S.C., Tauber, A., Wilber, W.D., Lareau, R.T., Brandle, C.D., Berkstresser, G.W., Ven Graitis, A.J., Potrepka, D.M., Budnick, J.I., Wu, J.Z.: New substrates for HTSC microwave devices. *IEEE Trans. Appl. Supercond.* **7**, 1766–1768 (1997)
- [4] Kumar, A., Podraza, N.J., Denev, S., Li, J., Martin, L.W., Chu, Y.-H., Ramesh, R., Collins, R.W., Gopalan, V.: Linear and nonlinear optical properties of multifunctional  $\text{PbVO}_3$  thin films. *Appl. Phys. Lett.* **92**, 231915 (2008)
- [5] Krockenberger, Y., Uchida, M., Takahashi, K.S., Nakamura, M., Kawasaki, M., Tokura, Y.: Growth of superconducting  $\text{Sr}_2\text{RuO}_4$  thin films. *Appl. Phys. Lett.* **97**, 082502 (2010)
- [6] Verma, A., Raghavan, S., Stemmer, S., Jena, D.: Ferroelectric transition in compressively strained  $\text{SrTiO}_3$  thin films. *Appl. Phys. Lett.* **107**, 192908 (2015)
- [7] Goian, V., Langenberg, E., Marcano, N., Bovtun, V., Maurel, L., Kempa, M., Prokscha, T., Kroupa, J., Algarabel, P.A., Pardo, J.A., Kamba, S.: Spin-phonon coupling in epitaxial  $\text{Sr}_{0.6}\text{Ba}_{0.4}\text{MnO}_3$  thin films. *Phys. Rev. B* **95**, 075126 (2017)
- [8] Sumiya, M., Chikyow, T., Sasahara, T., Yoshimura, K., Ohta, J., Fujioka, H., Tagaya, S., Ikeya, H., Koinuma, H., Fuke, S.: Epitaxial growth of GaN film on  $(\text{La,Sr})(\text{Al,Ta})\text{O}_3$  (111) substrate by metalorganic chemical vapor deposition. *Jpn. J. Appl. Phys.* **41**, 5038 (2002)
- [9] Kojima, K.M., Hiraiishi, M., Koda, A., Okabe, H., Takeshita, S., Li, H., Kadono, R., Tanaka, M.M., Shoji, M., Uchida, T., Suzuki, S.Y.: Development of general purpose  $\mu\text{SR}$  spectrometer ARTEMIS at S1 experimental area, MLF J-PARC. *JPS Conf. Proc.* **21**, 011062 (2018)

- [10] Giannozzi, P., Baroni, S., Bonini, N., Calandra, M., Car, R., Cavazzoni, C., Ceresoli, D., Chiarotti, G.L., Cococcioni, M., Dabo, I., Dal Corso, A., de Gironcoli, S., Fabris, S., Fratesi, G., Gebauer, R., Gerstmann, U., Gougoussis, C., Kokalj, A., Lazzeri, M., Martin-Samos, L., Marzari, N., Mauri, F., Mazzarello, R., Paolini, S., Pasquarello, A., Paulatto, L., Sbraccia, C., Scandolo, S., Sclauzero, G., Seitsonen, A.P., Smogunov, A., Umari, P., Wentzcovitch, R.M.: QUANTUM ESPRESSO: a modular and open-source software project for quantum simulations of materials. *J. Phys.: Condens. Matter* **21**, 395502 (2009)
- [11] Giannozzi, P., Andreussi, O., Brumme, T., Bunau, O., Nardelli, M.B., Calandra, M., Car, R., Cavazzoni, C., Ceresoli, D., Colonna, N., Carnimeo, I., Dal Corso, A., de Gironcoli, S., Delugas, P., DiStasio, R.A., Ferretti, A., Floris, A., Fratesi, G., Fugallo, G., Gebauer, R., Gerstmann, U., Giustino, F., Gorni, T., Jia, J., Kawamura, M., Ko, H.-Y., Kokalj, A., Küçükbenli, E., Lazzeri, M., Marsili, M., Marzari, N., Mauri, F., Nguyen, N.L., Nguyen, H.-V., Otero-de-la-Roza, A., Paulatto, L., Poncé, S., Rocca, D., Sabatini, R., Santra, B., Schlipf, M., Seitsonen, A.P., Smogunov, A., Timrov, I., Thonhauser, T., Umari, P., Vast, N., Wu, X., Baroni, S.: Advanced capabilities for materials modelling with quantum espresso. *J. Phys.: Condens. Matter* **29**, 465901 (2017)
- [12] Calderon, C.E., Plata, J.J., Toher, C., Oses, C., Levy, O., Fornari, M., Natan, A., Mehl, M.J., Hart, G., Buongiorno Nardelli, M., Curtarolo, S.: The AFLOW standard for high-throughput materials science calculations. *Comput. Mater. Sci.* **108**, 233–238 (2015)
- [13] CRYSTAL GmbH: LSAT data sheet. [https://crystal-gmbh.com/shared/downloads/datenblaetter/substrates\\_de/LSAT\\_Lanthanum\\_Aluminate\\_Strontium\\_Aluminum\\_Tantalate.pdf](https://crystal-gmbh.com/shared/downloads/datenblaetter/substrates_de/LSAT_Lanthanum_Aluminate_Strontium_Aluminum_Tantalate.pdf)
- [14] Van de Walle, A.: Multicomponent multisublattice alloys, nonconfigurational entropy and other additions to the Alloy Theoretic Automated Toolkit. *Calphad* **33**, 266–278 (2009)
- [15] Hayano, R.S., Uemura, Y.J., Imazato, J., Nishida, N., Yamazaki, T., Kubo, R.: Zero- and low-field spin relaxation studied by positive muons. *Phys. Rev. B* **20**, 850–859 (1979)
- [16] Ito, T.U., Higemoto, W., Matsuda, T.D., Koda, A., Shimomura, K.: Shallow donor level associated with hydrogen impurities in undoped BaTiO<sub>3</sub>. *Appl. Phys. Lett.* **103**, 042905 (2013)
- [17] Salman, Z., Prokscha, T., Amato, A., Morenzoni, E., Scheuermann, R., Sedlak, K., Suter, A.: Direct spectroscopic observation of a shallow hydrogenlike donor state in insulating SrTiO<sub>3</sub>. *Phys. Rev. Lett.* **113**, 156801 (2014)
- [18] Vieira, R.B.L., Vilão, R.C., Marinopoulos, A.G., Gordo, P.M., Paixão, J.A., Alberto, H.V., Gil, J.M., Weidinger, A., Lichti, R.L., Baker, B., Mengyan, P.W.,



- Lord, J.S.: Isolated hydrogen configurations in zirconia as seen by muon spin spectroscopy and ab initio calculations. *Phys. Rev. B* **94**, 115207 (2016)
- [19] Ito, T.U., Higemoto, W., Koda, A., Shimomura, K.: Polaronic nature of a muonium-related paramagnetic center in SrTiO<sub>3</sub>. *Appl. Phys. Lett.* **115**, 192103 (2019)
- [20] Ito, T.U.: Hydrogen-Ti<sup>3+</sup> complex as a possible origin of localized electron behavior in hydrogen-irradiated SrTiO<sub>3</sub>. *e-J. Surf. Sci. Nanotech.* **20**, 128–134 (2022)
- [21] Storchak, V.G., Prokof'ev, N.V.: Quantum diffusion of muons and muonium atoms in solids. *Rev. Mod. Phys.* **70**, 929–978 (1998)
- [22] Ito, T.U., Higemoto, W., Shimomura, K.: Understanding muon diffusion in perovskite oxides below room temperature based on harmonic transition state theory. *Phys. Rev. B* **108**, 224301 (2023)
- [23] Ito, T.U., Kadono, R.: Distinguishing ion dynamics from muon diffusion in muon spin relaxation. *J. Phys. Soc. Jpn.* **93**, 044602 (2024)
- [24] Hempelmann, R., Soetratmo, M., Hartmann, O., Wäppling, R.: Muon diffusion and trapping in proton conducting oxides. *Solid State Ionics* **107**, 269–280 (1998)
- [25] Ito, T.U., Koda, A., Shimomura, K., Higemoto, W., Matsuzaki, T., Kobayashi, Y., Kageyama, H.: Excited configurations of hydrogen in the BaTiO<sub>3-x</sub>H<sub>x</sub> perovskite lattice associated with hydrogen exchange and transport. *Phys. Rev. B* **95**, 020301 (2017)